NASA CONTRACTOR REPORT

NASA CR-2087

NASA CR-2087

THE EFFECT OF ANGLE OF ATTACK ON THE BUCKLING OF MARS ENTRY AEROSHELLS

by Gerald A. Cohen

Prepared by
STRUCTURES RESEARCH ASSOCIATES
Laguna Beach, Calif. 92651
for Langley Research Center

NATIONAL AERONAUTICS AND SPACE ADMINISTRATION • WASHINGTON, D. C. • FEBRUARY 1973

1. Report No.	2. Government Accession No.	3. Recipient's Catalog No.
NASA CR-2087		

4. Title and Subtitle	5. Report Date
THE EFFECT OF ANGLE OF ATTACK ON THE BUCKLING OF MARS ENTRY AEROSHELLS	February 1973
	6. Performing Organization Code
7. Author(s)	8. Performing Organization Report No.
Gerald A. Cohen	
9. Performing Organization Name and Address	10. Work Unit No.
Structures Research Associates 465 Forest Avenue, Suite J Laguna Beach, CA	124-08-20-04-00
	11. Contract or Grant No.
	NAS1-10091
12. Sponsoring Agency Name and Address	13. Type of Report and Period Covered
National Aeronautics and Space Administration Washington, D.C. 20546	Contractor report
	14. Sponsoring Agency Code

15. Supplementary Notes

This is a companion report to NASA CR-2085 and NASA CR-2086

16. Abstract

THE BUCKLING MODES OF FOUR OPTIMIZED MARS ENTRY AEROSHELL CONFIGURATIONS AT ANGLE-OF-ATTACK LOADINGS HAVE BEEN CALCULATED. THE CONFIGURATIONS TREATED (120° AND 140° BLUNTED SANDWICH AND RING-STIFFENED CONES, THE 140° RING-STIFFENED CONE BEING A PROTOTYPE VIKING AEROSHELL) WERE OBTAINED IN PREVIOUS STUDIES. THE ANALYSIS IS BASED ON EXPERIMENTAL PRESSURE DISTRIBUTIONS AND WAS PERFORMED WITH THE AID OF A BUCKLING DIGITAL COMPUTER PROGRAM WHICH TREATS GENERAL ASYMMETRIC LINEARIZED PREBUCKLING STATES OF BRANCHED SHELLS OF REVOLUTION. ONLY ZEROTH AND FIRST HARMONIC PRESSURE COMPONENTS ARE TREATED, THESE BEING CONSTRUCTED FROM WINDWARD AND LEEWARD MERIDIAN PRESSURE DATA AT A MACH NUMBER OF 4.63.

THE RESULTS SHOWED A RATHER SMALL EFFECT OF THE UNSYMMETRICAL PRESSURE COMPONENT ON BUCKLING FOR ANGLES OF ATTACK UP TO 15°. FOR EXAMPLE, FOR THE VIKING AEROSHELL, THE EFFECT OF THE $n = 1$ LOAD COMPONENT IS TO REDUCE THE CRITICAL NORMAL SHOCK STAGNATION PRESSURE BY ONLY 3.9% AND 6.3% FOR ANGLES OF ATTACK OF 10° AND 15°, RESPECTIVELY. COMPARISON OF THE RESULTS FOR THE 120° CONES TO PREVIOUS RESULTS INDICATES THAT THE COMMON PROCEDURE OF BASING THE DESIGN ON A SYMMETRIZED PRESSURE DISTRIBUTION OF THE WINDWARD MERIDIAN IS A CONSERVATIVE APPROACH.

17. Key Words (Suggested by Author(s))	18. Distribution Statement
Linear asymmetric buckling, angle of attack, shell of revolution, Viking aeroshell, Mars entry aeroshells	Unclassified - Unlimited

19. Security Classif. (of this report)	20. Security Classif. (of this page)	21. No. of Pages	22. Price*
Unclassified	Unclassified	20	$3.00

*For sale by the National Technical Information Service, Springfield, Virginia 22151

CONTENTS

THE EFFECT OF ANGLE OF ATTACK ON THE BUCKLING OF MARS ENTRY AEROSHELLS

By Gerald A. Cohen
Structures Research Associates, Laguna Beach, California

SUMMARY

The buckling modes of four optimized Mars entry aeroshell configurations at angle-of-attack loadings have been calculated. The configurations treated (120° and 140° blunted sandwich and ring-stiffened cones, the 140° ring-stiffened cone being a prototype Viking aeroshell) were obtained in previous studies. The anlysis is based on experimental pressure distributions and was performed with the aid of a buckling digital computer program which treats general asymmetric linearized prebuckling states of branched shells of revolution. Only zeroth and first harmonic pressure components are treated, these being constructed from windward and leeward meridian pressure data at a Mach number of 4.63.

The results showed a rather small effect of the unsymmetrical pressure component on buckling for angles of attack up to 15°. For example, for the Viking aeroshell, the effect of the n = 1 load component is to reduce the critical normal shock stagnation pressure by only 3.9% and 6.3% for angles of attack of 10° and 15°, respectively. Comparison of the results for the 120° cones to previous results indicates that the common procedure of basing the design on a symmetrized pressure distribution of the windward meridian is a conservative approach.

INTRODUCTION

In references 1-3 several optimum aeroshells designs are synthesized for a Mars entry capsule. In each case the structural weight is minimized with respect to buckling failure of the aeroshell based on assumed axisymmetric pressure distributions. In reference 1, 120° sandwich and ring-stiffened cone designs are synthesized using the symmetrized pressure distribution of the windward meridian obtained from theoretical flow field calculations at 9° angle of attack. In reference 2, a 140° sandwich cone is synthesized using a calculated pressure distribution for zero angle of attack. In reference 3, a 140° ring-stiffened cone for the Viking mission is synthesized using simply a uniform pressure distribution.

Recently, a computer program has been developed for the bifurcation buckling analysis of shells of revolution subjected to general asymmetric loads (designated as SRA 101 in refs. 4 and 5). The purpose of this study is to reanalyze, with the aid of this new program, the above-mentioned aeroshell designs using more realistic pressure distributions resulting from expected angles of attack at peak dynamic pressure during entry from a Martian orbit. Specifically, an angle of attack of 10° is considered for the 120° designs and the 140° sandwich design, and 10° and 15° are considered for the 140° ring-stiffened Viking design.

SYMBOLS

D	base diameter
n	circumferential harmonic number
p	local pressure
p_s	normal shock stagnation pressure
s	meridional distance measured from pole of spherical nose cap (figs. 2-8) or from base ring (figs. 9-12)
α	angle of attack

AEROSHELL CONFIGURATIONS AND LOADS

In figure 1 are shown the four configurations treated. Further details of these designs are given in references 1, 2 and 3. For the designs of reference 1, only the low temperature (300°F), low ballistic coefficient (0.32 slug/ft^2) 120° conical designs are considered. Of the two aeroshell designs of reference 3, only the light (35 lb) base ring design is considered. In contrast to the 120° cone and 140° sandwich cone designs (refs. 1 and 2), which have a 19 foot base diameter and a bluntness ratio (spherical nose radius to base radius) of 0.25, the 140° ring-stiffened Viking cone (ref. 3) has an 11.5 foot base diameter and a bluntness ratio of 0.50.

The experimental pressure distribution for blunt 120° cones at a Mach number of 4.63 and 10° angle of attack was taken from table III of reference 6. Experimental pressure distributions for blunt 140° cones at a Mach number of 4.63 and 10° and 15° angle of attack were taken from table IV of reference 7. Data for the windward and leeward meridians (reproduced here in fig. 2) was used to calculate zeroth and first harmonic pressure loadings, all other harmonics being ignored.

For each of these harmonics, linearized prebuckling states for a normal shock stagnation pressure p_s of 1 psi were calculated by the computer program SRA 100 (ref. 5). In this calculation the pressure loading is reacted by the distributed inertial loads of the aeroshell accelerating in a rigid body mode. The critical value of the normal shock stagnation pressure was then calculated for this asymmetric prebuckling state by SRA 101.*

RESULTS

19 Foot Aeroshells (Refs. 1 and 2)

In general, for blunt aeroshells the buckling response of the shell section forward of the payload ring is negligible. Therefore, the computer models of the 120° cones and the 140° sandwich cone extend only from the payload ring to the base ring. For these cones, estimates of the payload and nose section masses were lumped into the payload ring by the artifice of increasing its mass density. Also, the resultant force and moment of the pressure distribution on the nose section were applied as effective loads at the payload ring. In all cases, the stiffness of the payload attachment was neglected.

Calculated critical values of p_s (psi) are shown in the table below, in which α represents angle of attack and n represents circumferential harmonic number. Buckling mode harmonics for which the normal displacement amplitude is greater than 1/2 of 1% of the amplitude of the dominant harmonic are given in parentheses. Also shown are previous results from references 1 and 2.

Aeroshell	$\alpha = 10°$ (n = 0 pressure component only)	$\alpha = 10°$ (n = 0 and n = 1 pressure components)	$\alpha = 9°$ (ref. 1)	$\alpha = 0°$ (ref. 2)
120° Sand. Cone	7.228 (2)	7.221 (2,3)	6.69 (2)	--
120° R.S. Cone	7.10 (5)	6.90 (2-8)	6.38 (5)	--
140° Sand. Cone	5.22 (6)	5.02 (3-8)	--	5.88 (5)

The results from reference 1 are based on nonlinear buckling analyses using an axisymmetric pressure distribution with meridional variation equal to that of the windward meridian calculated at 9° angle of attack. The nonlinear effect for the 120° cones is small, and comparison of figure 11 of reference 1 with figure 2 shows that, in spite of differences in Mach number, specific heat ratio, and angle of attack, the two pressure distributions are very much alike.

*Dead pressure loading was assumed.

This comparison therefore suggests that the procedure of designing the shell on the basis of the windward meridian pressure distribution is conservative.

The result shown from reference 2 is based on a nonlinear prebuckling analysis using a calculated axisymmetric pressure distribution at zero angle of attack. As shown, the present linear results are below that nonlinear result. This is due to the beneficial effect of the prebuckling nonlinearity, as noted in reference 2.

The corresponding prebuckling stress resultants (for p_s = 1 psi) and the normal displacements of the buckling modes are shown in figures 3 through 8. In these figures, the meridional distance s is measured from the pole of the spherical nose cap, and the curves start at the payload ring and terminate at the base ring. It may be of interest to note that for large angle cones such as these, the n = 1 shear stress resultant and meridional stress resultant amplitudes are approximately equal in magnitude. (In figures 3, 5 and 7, the curves for these two variables are practically indistinguishable.) Also, since the pressure loading has an axial plane of symmetry, there exist uncoupled symmetric and antisymmetric buckling modes. However, in all cases studied, these two buckling modes are essentially identical. As has been noted in reference 1, the inextensional buckling mode for the 120° sandwich cone (fig. 4) results because in this case the base ring is slightly undersized.

Viking Aeroshell (Ref. 3)

For this design, the payload ring is considerably farther aft than for the 19 foot designs. In this case the payload attachment radius is 0.487 of the base ring attachment radius, whereas the corresponding ratios are 0.30 for the 120° cones and 0.35 for the 140° sandwich cone. In contrast to the preceding analyses, it was therefore thought desirable to model at least part of the shell forward of the payload ring. On the other hand, the blunt cone models used in references 6 and 7 had a bluntness ratio of 0.25, so that strictly speaking the experimental pressure data does not apply to the Viking shell with a bluntness ratio of 0.50. In view of these considerations, the shell was modeled from the base ring up to the cone-sphere juncture. The experimental pressure at a parallel circle on the conical part of the wind-tunnel model is assumed to apply to the computer model at the corresponding parallel circle with the same ratio of radius to base radius.* Because negligible buckling response is expected in the deleted spherical portion, simple support boundary conditions were imposed at the artificial edge created in the model.

---

*For the computer model, the base radius was taken as the base ring attachment radius, i.e., 64.6 in.

Because of the large number of rings in the aeroshell and limitations due to current dimensioning of the computer programs involved, it was convenient to redistribute in the computer model several rings over the stringer-stiffened section of the shell. As noted in reference 1, a similar redistribution of rings was necessary in the model of the 120° ring-stiffened cone. Although this redistribution changes the local instability characteristics of the aeroshell, it has negligible effect on its general instability mode.

Calculated critical values of p_s (psi) and corresponding buckling mode harmonics for this model are shown in the table below.*

Angle-of-attack	n = 0 pressure component only	n = 0 and n = 1 pressure components
10°	4.85 (6)	4.66 (4-9)
15°	4.89 (6)	4.58 (4-9)

The corresponding prebuckling stress resultants (for p_s = 1 psi) and the normal displacements of the buckling modes are shown in figures 9 through 12. In these figures, the meridional distance s is measured from the base ring and the curves terminate at the cone-sphere juncture. The large discontinuity in the prebuckling stress resultants (figs. 9 and 11) occurs at the payload ring (s = 35.2 in). As expected, the buckling response forward of the payload ring is very small.

CONCLUSIONS

A newly developed computer program has been used to calculate the buckling modes of four blunt conical aeroshells, including a prototype Viking aeroshell, at angle-of-attack loadings. Two essential conclusions emerge from this study.

(1) For angles of attack up to 15°, the effect of the unsymmetrical prebuckling component is rather small. For the Viking shell, this component reduces the critical pressure due solely to the axisymmetric component by only 6.3% at 15° angle of attack.

(2) The procedure of the designing the aeroshell based on the symmetrized pressure distribution of the windward meridian appears to be conservative. For the 120° conical aeroshells, calculations using this procedure (ref. 1) underestimated the critical pressure by roughly 7.5%.

---

*For uniform pressure loading reacted at the payload ring, a critical pressure of 4.73 psi (based on linear prebuckling) is given in reference 3.

REFERENCES

1. Cohen, Gerald A.; Foster, Richard M.; and Dowty, James R.: Synthesis of Optimum Structural Designs for Conical and Tension Shell Mars Entry Capsules. NASA CR-1365, 1969.

2. Cohen, Gerald A.: Evaluation of Configuration Changes on Optimum Structural Designs for a Mars Entry Capsule. NASA CR-1414, 1969.

3. Heard, Walter L., Jr.; and Anderson, Melvin S.: Design, Analysis, and Tests of a Structural Prototype Viking Aeroshell. Part I - Aeroshell Design and Analysis. AIAA paper 72-370, presented at the AIAA/ASME/SAE 13th Structures, Structural Dynamics and Materials Conference (San Antonio), April 1972.

4. Cohen, Gerald A.: Computer Analysis of Ring-Stiffened Shells of Revolution. NASA CR-2085, 1973.

5. Cohen, Gerald A.: User Document for Computer Programs for Ring-Stiffened Shells of Revolution. NASA CR-2086, 1973.

6. Stallings, Robert L., Jr.; and Tudor, Dorothy H.: Experimental Pressure Distributions on a 120° Cone at Mach Numbers from 2.96 to 4.63 and Angles of Attack from 0° to 20°. NASA TN D-5054, 1969.

7. Campbell, James F.; and Tudor, Dorothy H.: Pressure Distributions on 140°, 160°, and 180° Cones at Mach Numbers from 2.30 to 4.63 and Angles of Attack from 0° to 20°. NASA TN D-5204, 1969.

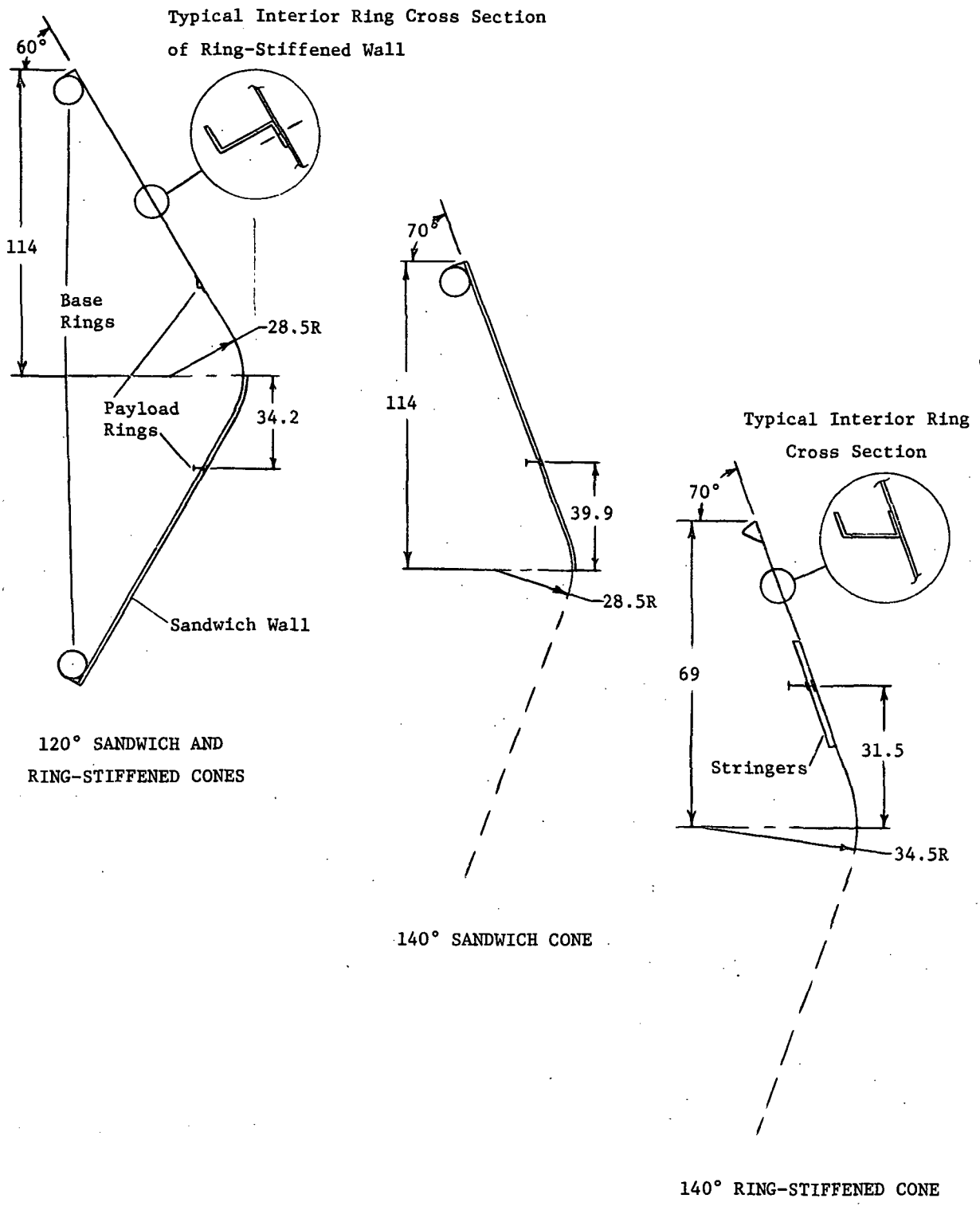

FIGURE 1. AEROSHELL CONFIGURATIONS
(Dimensions in inches)

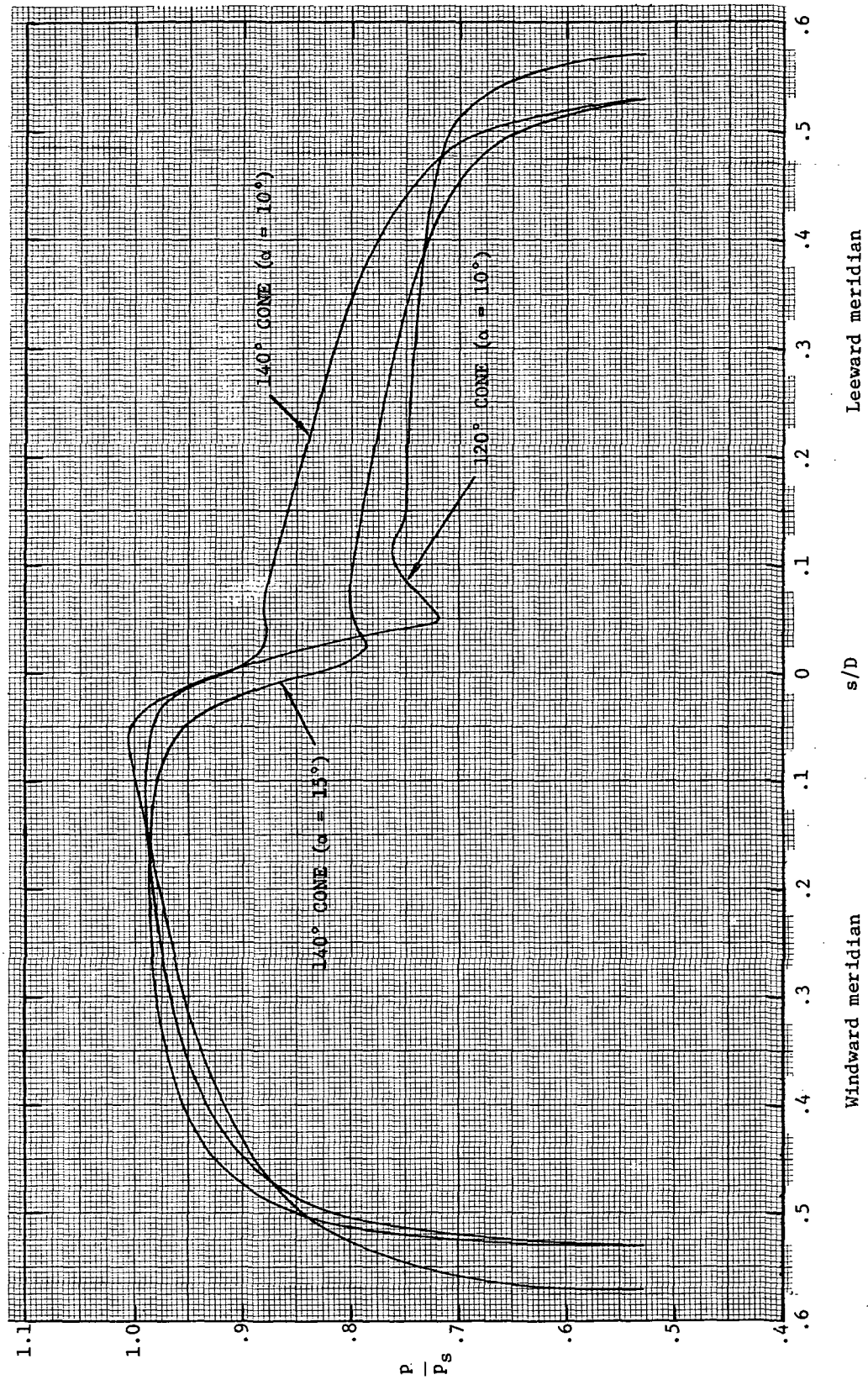

FIGURE 2. PRESSURE DISTRIBUTIONS AT ANGLE OF ATTACK
[FROM REFS. 6 AND 7]

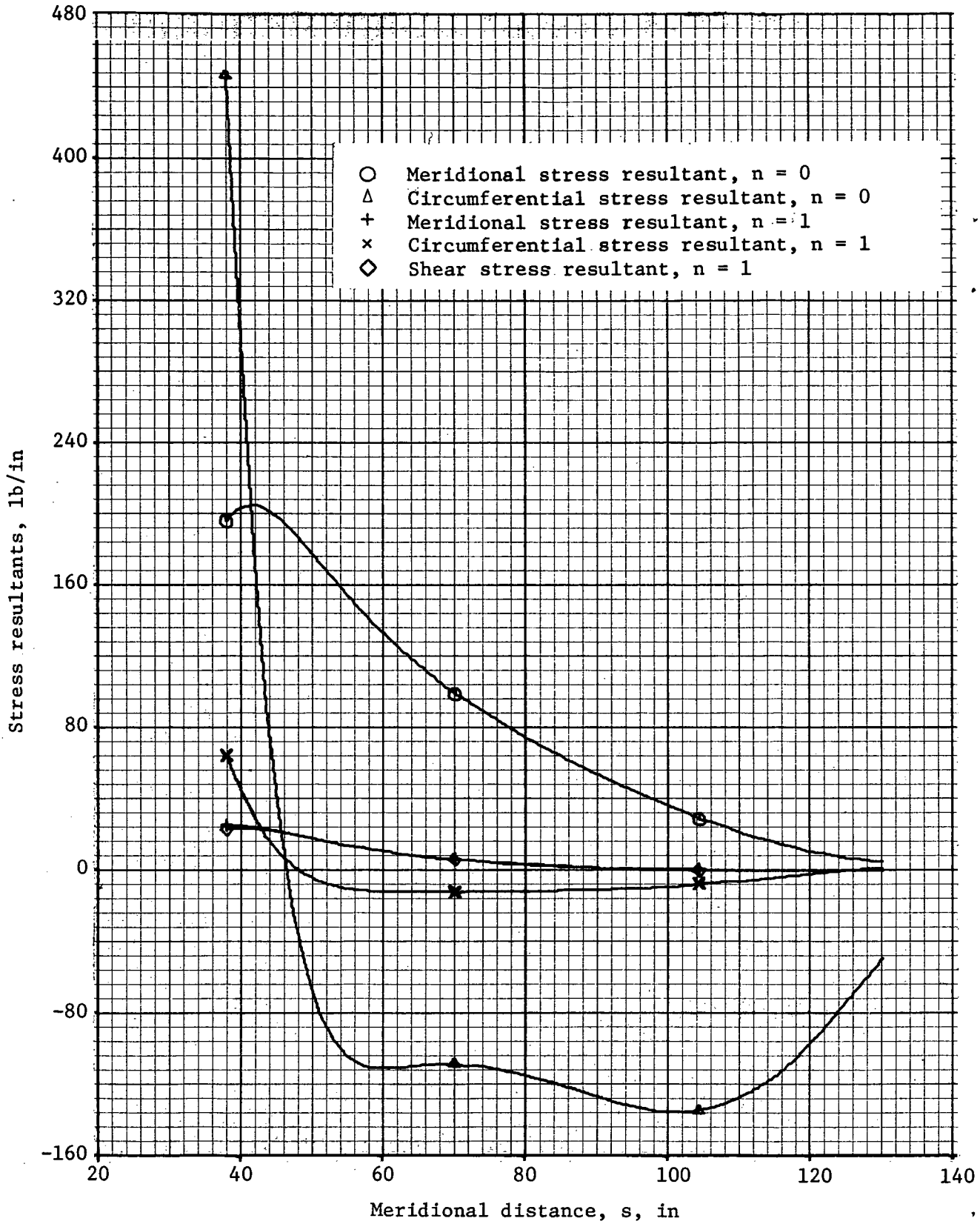

FIGURE 3. PREBUCKLING STRESS RESULTANTS, 120° SANDWICH CONE

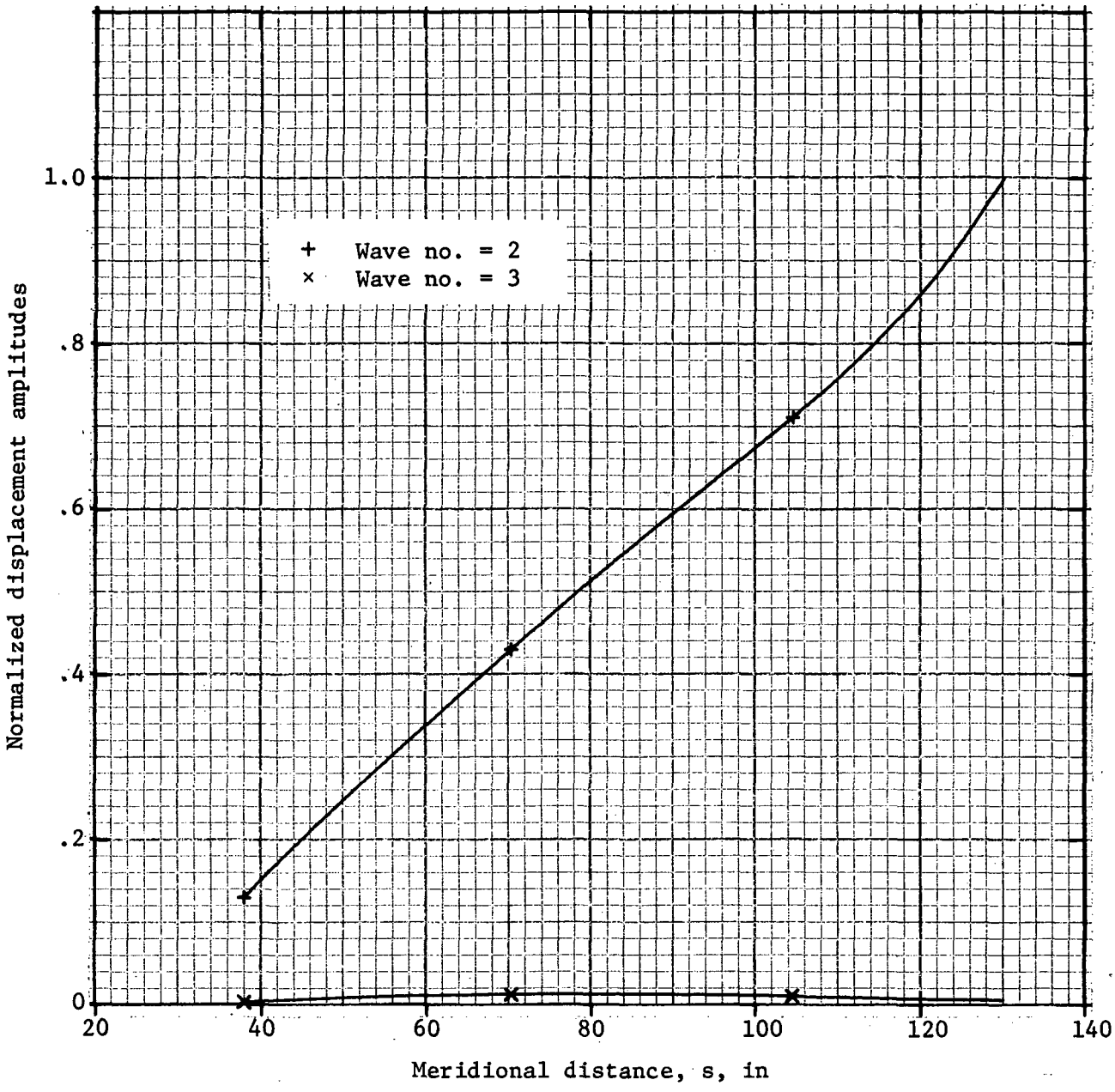

FIGURE 4. BUCKLING MODE DISPLACEMENTS, 120° SANDWICH CONE (CRITICAL p_s = 7.221 PSI)

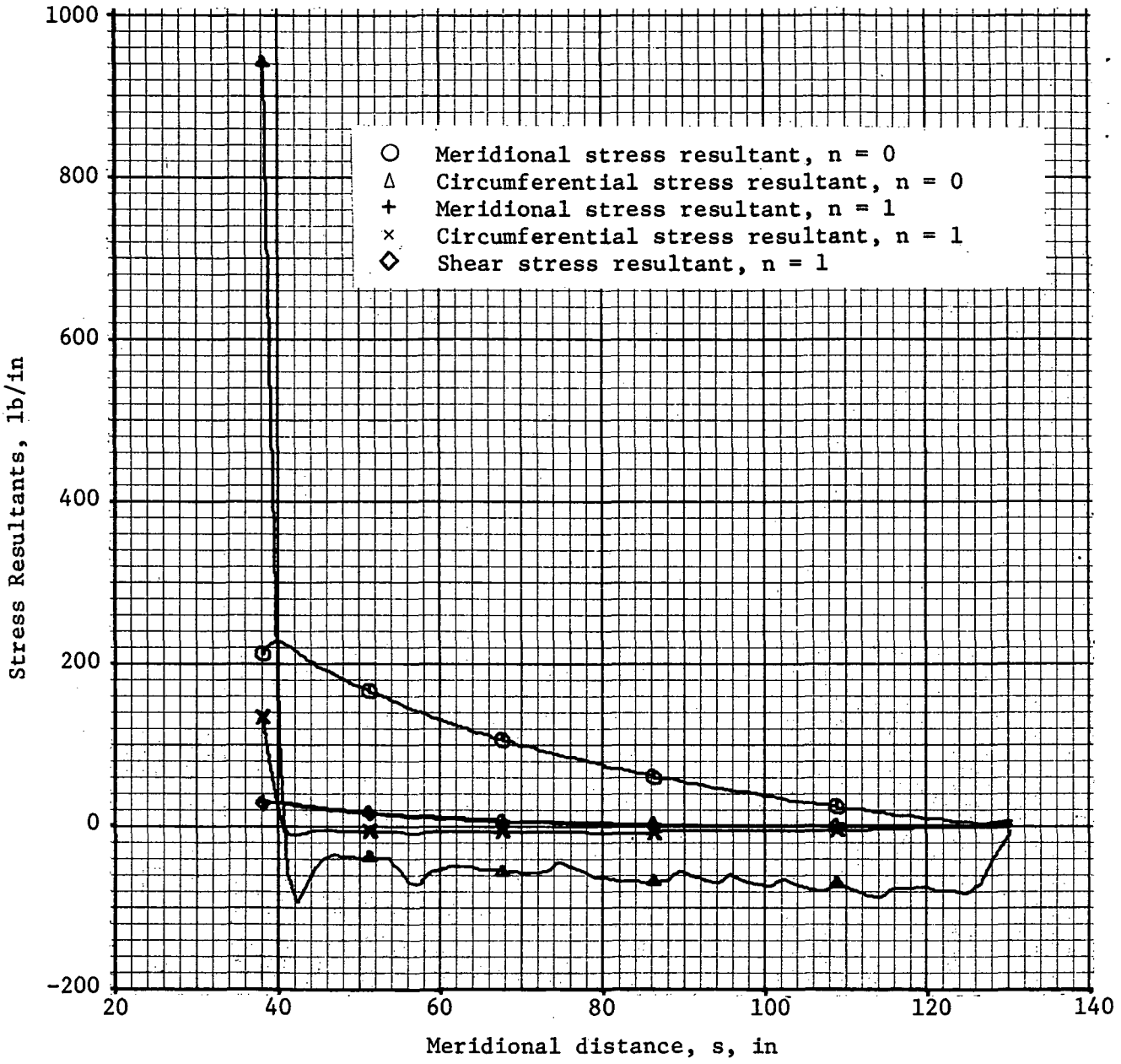

FIGURE 5. PREBUCKLING STRESS RESULTANTS, 120° RING-STIFFENED CONE

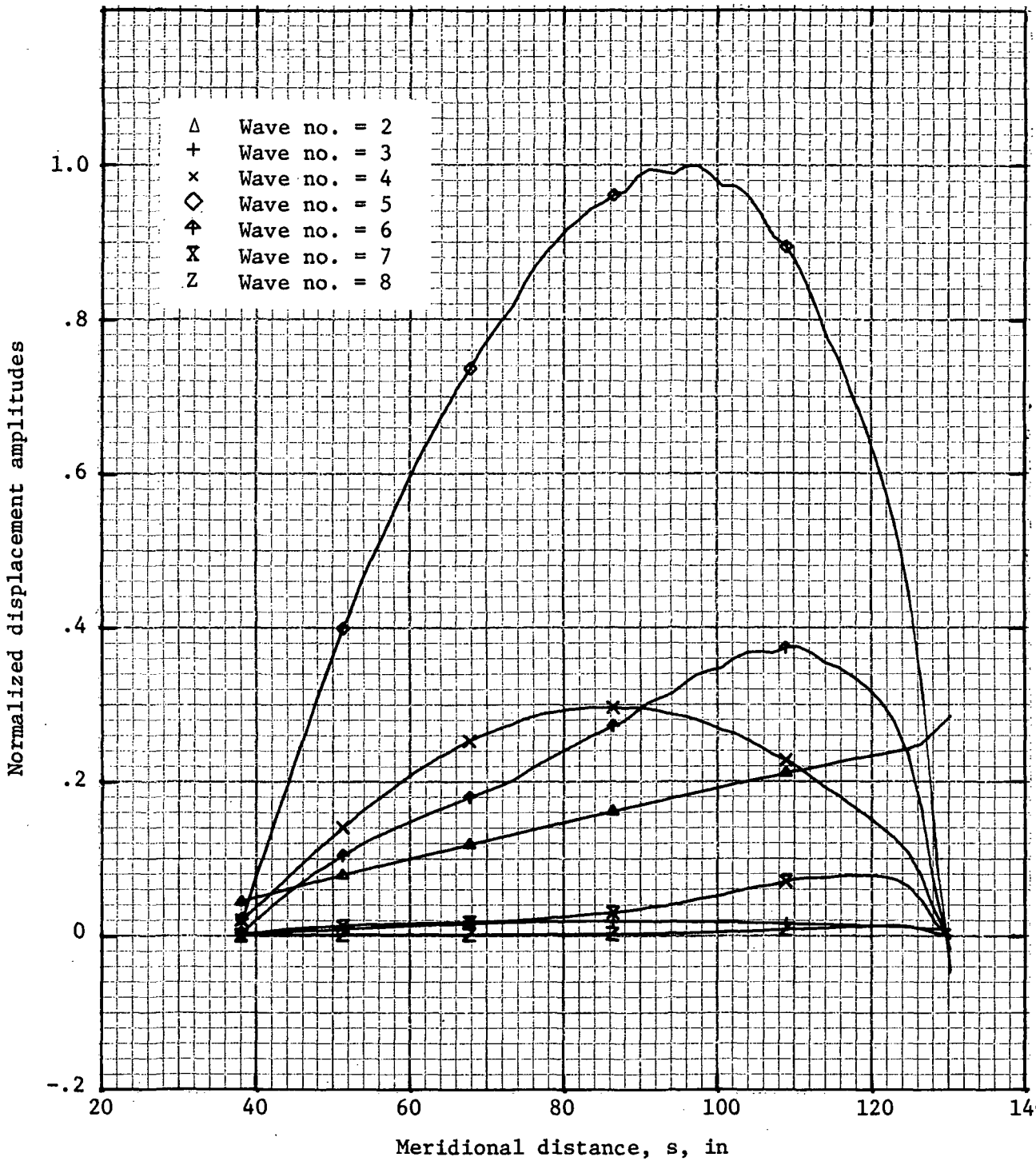

FIGURE 6. BUCKLING MODE DISPLACEMENTS, 120° RING-STIFFENED CONE (CRITICAL p_s = 6.90 PSI)

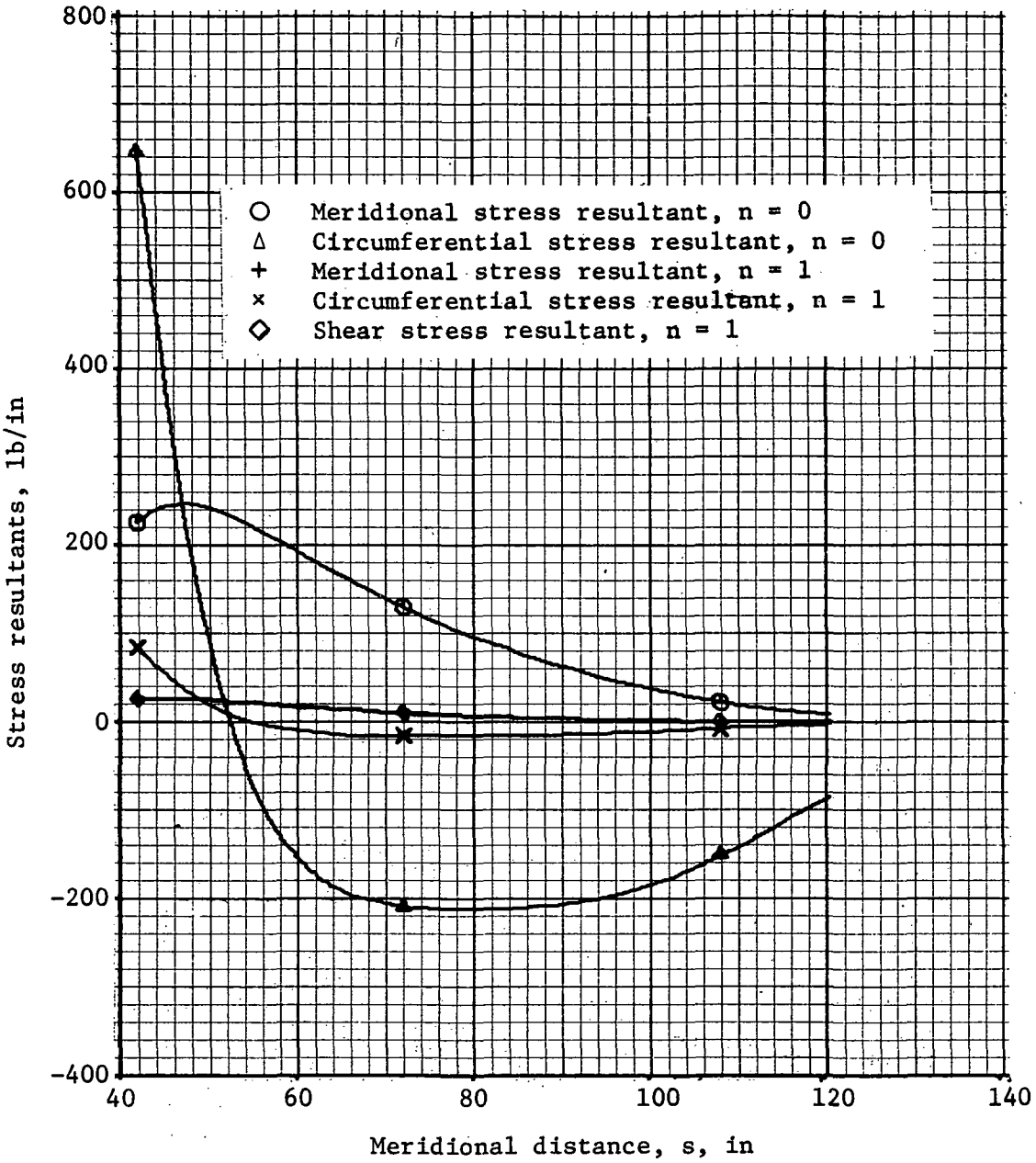

FIGURE 7. PREBUCKLING STRESS RESULTANTS, 140° SANDWICH CONE

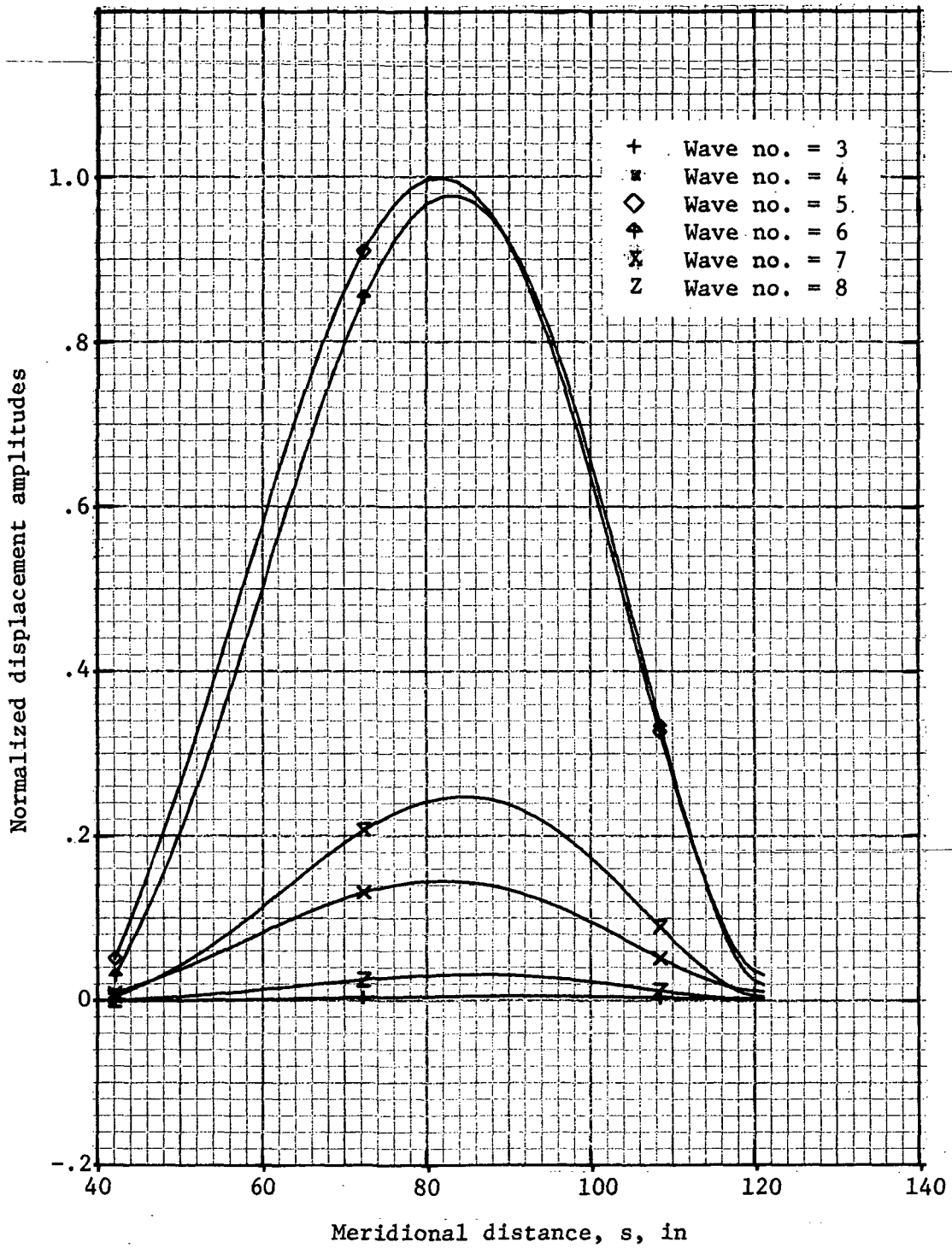

FIGURE 8. BUCKLING MODE DISPLACEMENTS, 140° SANDWICH CONE (CRITICAL p_s = 5.02 PSI)

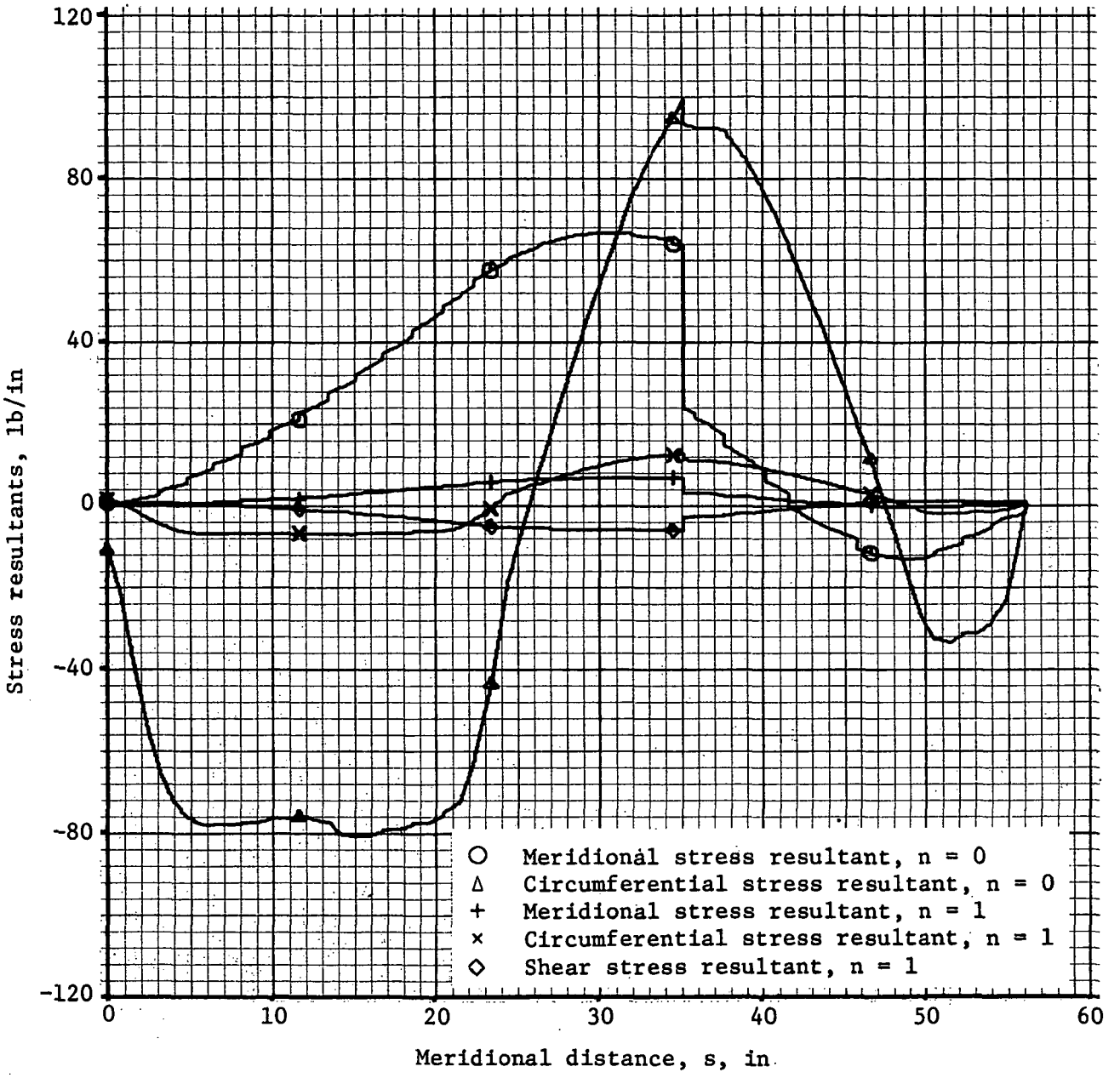

FIGURE 9. PREBUCKLING STRESS RESULTANTS, VIKING AEROSHELL, $\alpha = 10°$

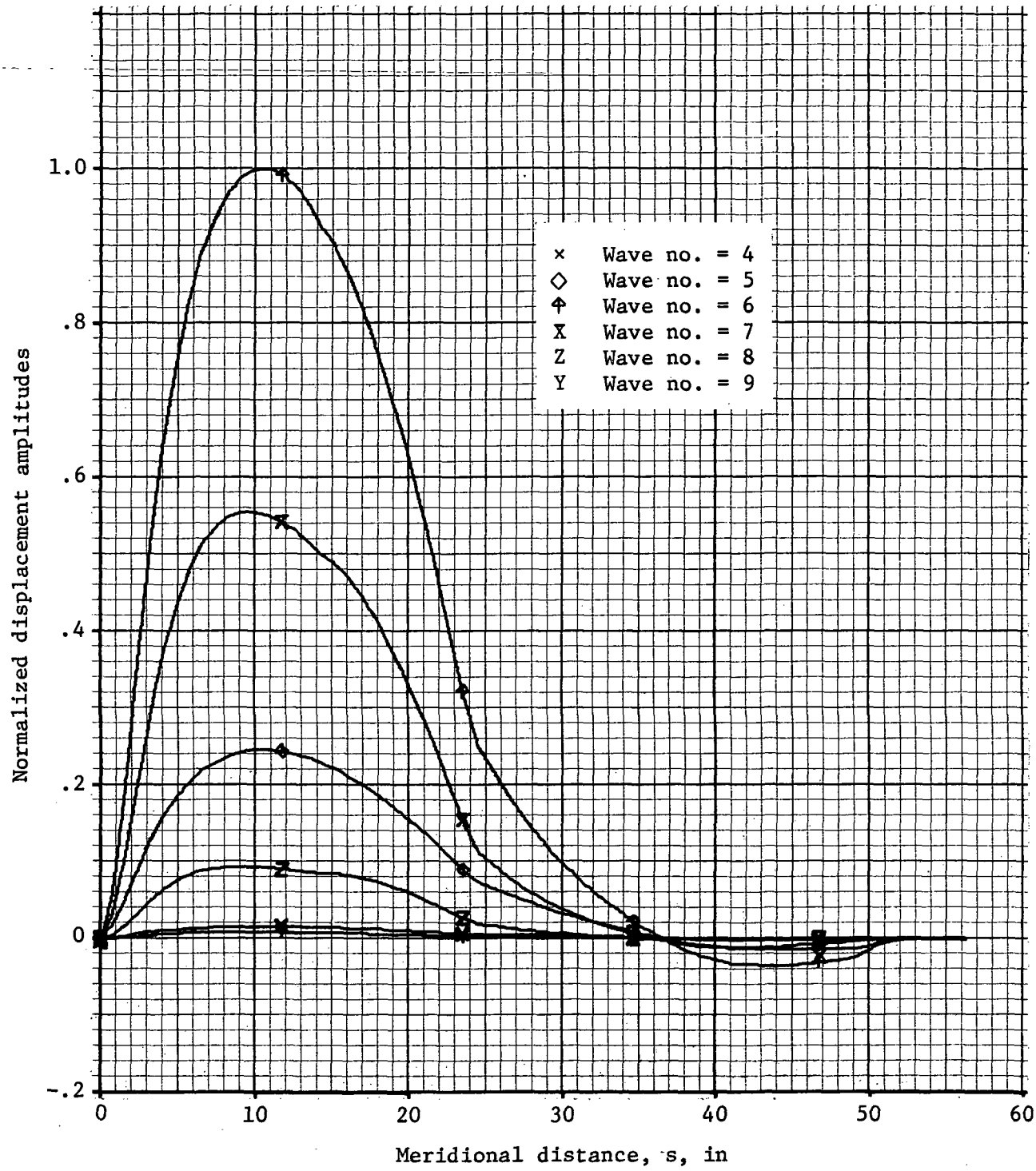

FIGURE 10. BUCKLING MODE DISPLACEMENTS, VIKING AEROSHELL, $\alpha = 10°$ (CRITICAL $p_s = 4.66$ PSI)

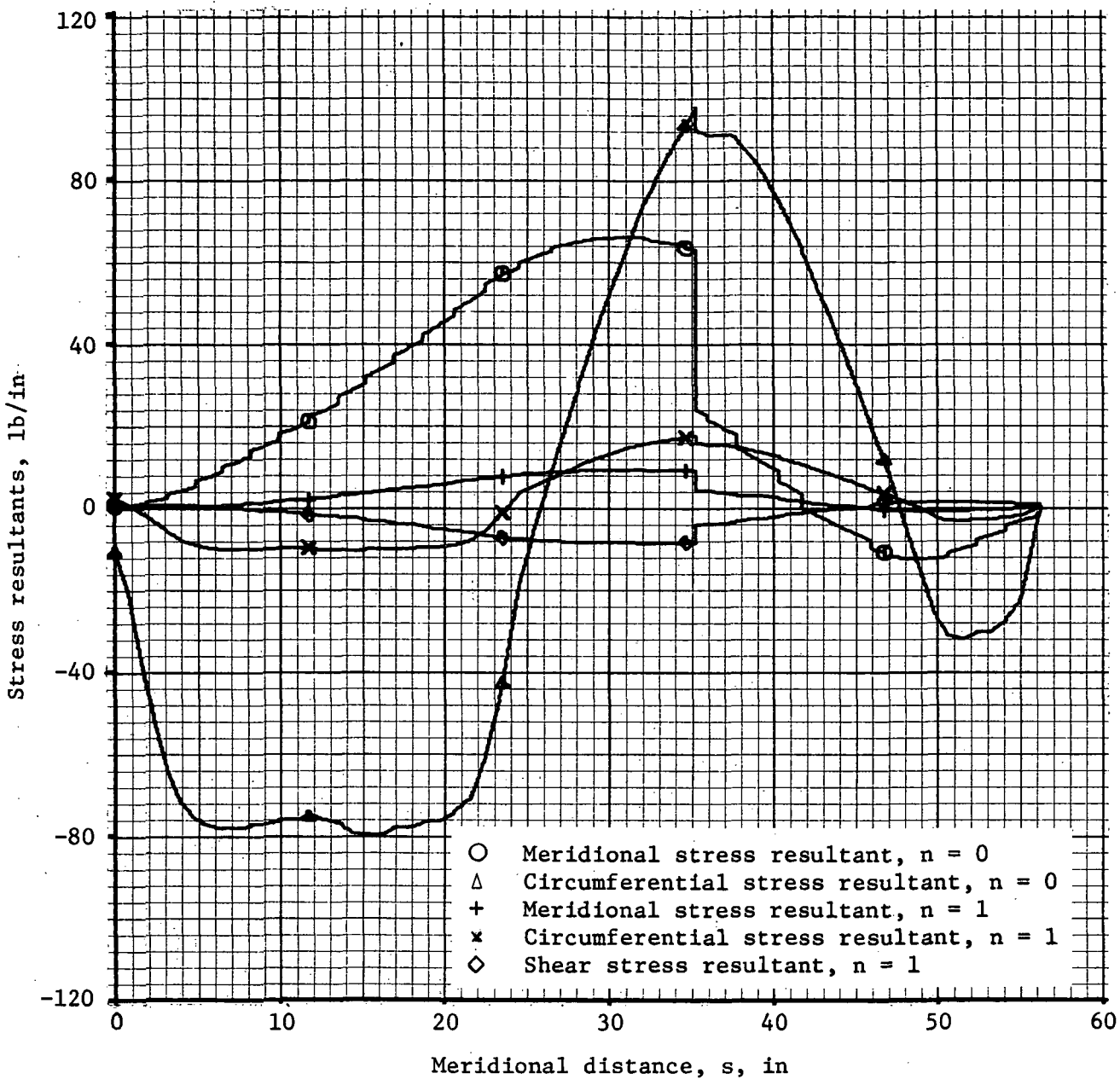

FIGURE 11. PREBUCKLING STRESS RESULTANTS, VIKING AEROSHELL, $\alpha = 15°$

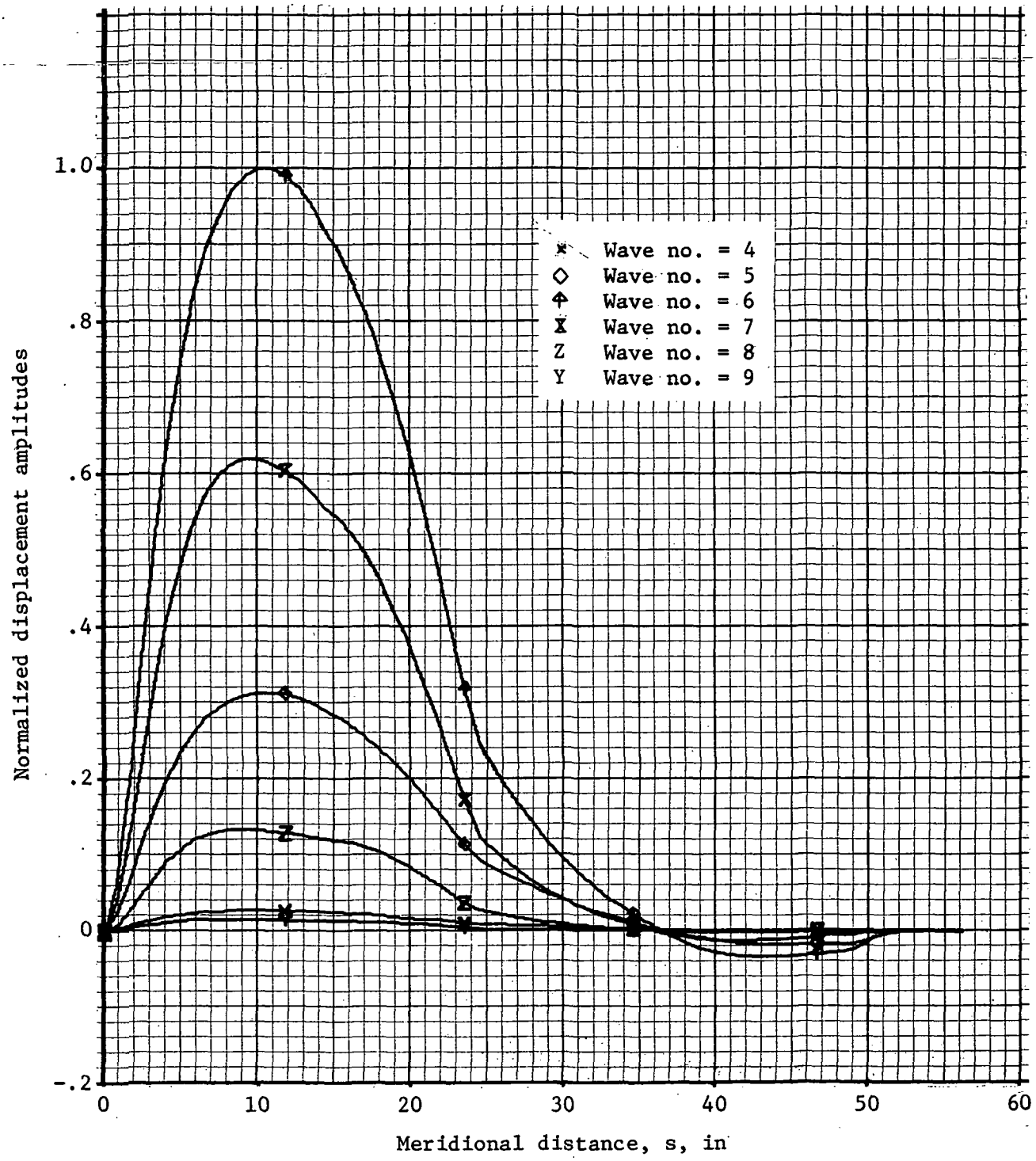

FIGURE 12. BUCKLING MODE DISPLACEMENTS, VIKING AEROSHELL, $\alpha = 15°$ (CRITICAL $p_s = 4.58$ PSI)

"The aeronautical and space activities of the United States shall be conducted so as to contribute . . . to the expansion of human knowledge of phenomena in the atmosphere and space. The Administration shall provide for the widest practicable and appropriate dissemination of information concerning its activities and the results thereof."

—NATIONAL AERONAUTICS AND SPACE ACT OF 1958

NASA SCIENTIFIC AND TECHNICAL PUBLICATIONS

TECHNICAL REPORTS: Scientific and technical information considered important, complete, and a lasting contribution to existing knowledge.

TECHNICAL NOTES: Information less broad in scope but nevertheless of importance as a contribution to existing knowledge.

TECHNICAL MEMORANDUMS: Information receiving limited distribution because of preliminary data, security classification, or other reasons. Also includes conference proceedings with either limited or unlimited distribution.

CONTRACTOR REPORTS: Scientific and technical information generated under a NASA contract or grant and considered an important contribution to existing knowledge.

TECHNICAL TRANSLATIONS: Information published in a foreign language considered to merit NASA distribution in English.

SPECIAL PUBLICATIONS: Information derived from or of value to NASA activities. Publications include final reports of major projects, monographs, data compilations, handbooks, sourcebooks, and special bibliographies.

TECHNOLOGY UTILIZATION PUBLICATIONS: Information on technology used by NASA that may be of particular interest in commercial and other non-aerospace applications. Publications include Tech Briefs, Technology Utilization Reports and Technology Surveys.

Details on the availability of these publications may be obtained from:

SCIENTIFIC AND TECHNICAL INFORMATION OFFICE

NATIONAL AERONAUTICS AND SPACE ADMINISTRATION

Washington, D.C. 20546